Solid State Science and Technology, Vol. 34, No. 1 (2026) 40-59
https://doi.org/10.66514/ssst34-1-40-59

Ionic Conduction and Electrochemical Performance of Propylene Carbonate-Plasticized PLA–$LiClO_4$ Polymer Electrolytes for EDLC Applications

Fairuzdzah Ahmad Lothfy[1,], Nur Ainul Mardhiyah Shahri Zaili[1], Nurul Infaza Talalah Ramli[1], Siti Zafirah Zainal Abidin[2]*

[1]Faculty of Applied Sciences, Universiti Teknologi MARA Pahang, Bandar Tun Abdul Razak Jengka, Pahang, Malaysia
[2]Faculty of Applied Sciences, Universiti Teknologi MARA, 40450 Shah Alam, Selangor, Malaysia

**Corresponding author (email: fairuzdzah@uitm.edu.my)*

(Received: 20 July 2026 / Revised: 6 August 2026 / Accepted: 24 August 2026 / Published online: 25 August 2026)

ABSTRACT

The transition to green energy technologies requires environmentally friendly electrolytes that can replace hazardous liquid systems while enabling rapid charge storage. This study investigates biodegradable solid polymer electrolytes based on a poly (lactic acid)–$LiClO_4$ matrix plasticized with 10–70 wt.% propylene carbonate for electric double-layer capacitor (EDLC) applications. Electrochemical and structural analyses showed that the electrolyte containing 30 wt.% propylene carbonates exhibited the best performance, achieving a room-temperature ionic conductivity of 1.69×10^{-3} S cm^{-1} due to a maximized free-ion fraction (65.71%) and enhanced polymer chain flexibility, along with a broad electrochemical stability window of 5.6 V. The fabricated EDLC demonstrated a maximum specific capacitance of 47.43 F g^{-1} at 1 mV s^{-1}, delivering an energy density of 3.12 Wh kg^{-1} and a power density of 173.61 W kg^{-1} at 5 mA g^{-1}. These results confirmed the potential of the developed electrolyte for sustainable, high-performance green energy storage applications in next-generation EDLCs.

Keywords: Polylactic acid; impedance; conductivity; cyclic voltammetry; galvanostatic charge-discharge

INTRODUCTION

The rapid growth of electric transportation and the increasing adoption of renewable energy technologies have intensified the demand for safe, efficient and sustainable energy storage systems. Batteries and other electrochemical energy storage technologies are expected to play a crucial role in the transition to low-carbon energy systems. Their applications span electric mobility, renewable energy integration, backup power systems and portable electronic devices [1]. Among the available electrochemical energy storage technologies, electric double-layer capacitors (EDLCs), a major class of supercapacitors,

are particularly attractive because of their high power density, rapid charge–discharge capability, excellent reversibility and long cycle life.

In contrast to rechargeable batteries, which rely on faradaic redox reactions and structural changes within electrode materials to store energy, EDLCs store energy through the reversible electrostatic adsorption of electrolyte ions at the electrode–electrolyte interface. This non-faradaic charge storage mechanism enables EDLCs to charge and discharge rapidly while maintaining excellent cycling stability over extended use. The effectiveness of this mechanism has been demonstrated in recent studies on polymer-electrolyte supercapacitors. For instance, a poly(N-acryloylglycinamide-co-vinyltriazole) (p(NAGA-co-VTZ)) supramolecular polymer hydrogel doped with carbonized and activated polypyrrole nanotubes was used as the electrolyte in an EDLC, achieving a specific capacitance of 282.62 F g^{-1} at a current density of 0.2 A g^{-1} and an areal capacitance of 316.86 mF cm^{-2} at a scan rate of 10 mV s^{-1} [2]. In another study, Nandhinilakshmi et al. (2024) reported that $LiClO_4$ which contains plasticized biopolymer electrolyte achieved a power density of 7,452 W kg^{-1} and an energy density of 165.6 Wh kg^{-1} at a current density of 3.6 A g^{-1} These findings demonstrate that both polymer and biopolymer electrolytes are capable of supporting rapid ion transport and high-rate electrochemical performance when they possess sufficient ionic conductivity and maintain good contact with the electrode. Among the various electrode materials used in EDLCs, activated carbon remains one of the most popular because of its high specific surface area, adjustable pore structure, chemical stability, relatively low cost and compatibility with a wide range of electrolytes. Its interconnected micro- and mesoporous network provides abundant sites for ion adsorption, facilitating efficient electric double-layer formation. Nevertheless, the electrochemical performance of activated carbon electrodes is influenced not only by the accessible surface area but also by factors such as ionic conductivity, ion size, electrolyte viscosity, electrode wettability and electrolyte resistance. Consequently, the properties of the electrolyte have a significant influence on the practical performance of EDLCs, particularly in terms of power density, rate capability and operating voltage stability.

Conventional liquid electrolytes generally offer high ionic conductivity and excellent electrode wetting, making them suitable for high-performance EDLCs. However, their use is often limited by issues such as electrolyte leakage, evaporation, flammability, corrosion and the need for more complex packaging. As a result, solid polymer electrolytes and gel polymer electrolytes have gained considerable attention as promising alternatives. These materials can serve as both ion-conducting electrolytes and separators while also minimizing leakage and providing greater mechanical flexibility. Recent review articles and experimental studies have further highlighted the potential of combining biodegradable polymer electrolytes with activated carbon electrodes to develop EDLCs that are not only safer but also more environmentally sustainable [4, 5]. Despite these advantages, solid polymer electrolytes generally exhibit lower ionic conductivity at room temperature than conventional liquid electrolytes. This is because ion transport depends on the movement of the polymer chains and is influenced by factors such as the degree of crystallinity, segmental mobility and ion association.

Poly(lactic acid) (PLA) has attracted considerable attention as a bio-based polymer host because it is derived from renewable resources, is easy to process, possesses good mechanical strength and is biodegradable under appropriate industrial composting

conditions. Despite these advantages, pure PLA exhibits relatively low ionic conductivity at room temperature due to its rigid molecular structure and limited segmental chain mobility, which hinder ion transport. To address this limitation, lithium salts have been incorporated into the PLA matrix to enhance its electrochemical properties. For example, a recent study on PLA–$LiClO_4$ solid polymer electrolyte films reported a maximum ionic conductivity of approximately 2.66×10^{-5} S cm^{-1} at the optimum $LiClO_4$ concentration, demonstrating that the addition of lithium salt significantly improves the ionic conductivity of the PLA-based electrolyte [6].

The incorporation of a plasticizer such as propylene carbonate (PC) can enhance ion transport by reducing intermolecular interactions between polymer chains, increasing the free volume and improving chain flexibility. These structural changes facilitate the dissociation of $LiClO_4$ into mobile Li^+ and ClO_4^- ions, thereby promoting ion migration through the polymer matrix. Nevertheless, the electrochemical performance of plasticized biopolymer electrolytes depends on several factors, including the chemical structure of the polymer host, salt concentration, plasticizer content, ion association and electrode structure. For example, Nandhinilakshmi et al. reported that a plasticized biopolymer electrolyte achieved an ionic conductivity of 2.02×10^{-2} S cm^{-1} and a power density of 7,452 W kg^{-1} at a current density of 3.6 A g^{-1} [3]. However, these performance metrics were obtained from a different biopolymer system with distinct plasticizers, electrode materials and testing conditions. As such, they serve as useful benchmarks rather than direct performance targets for PLA–$LiClO_4$ electrolytes. Likewise, an EDLC based on a fish gelatin/$LiClO_4$ polymer electrolyte achieved a specific capacitance of 28.2 F g^{-1} and exhibited stable performance over 150 charge–discharge cycles, highlighting the potential of biodegradable polymer electrolytes for non-faradaic energy storage [7].

Despite these advances, the effect of PC concentration on ion dissociation, free-ion formation, ion-pair interactions, ionic conductivity, impedance characteristics, electrochemical stability and overall EDLC performance in PLA–$LiClO_4$ electrolytes remains unclear. In particular, the relationship between the concentration of mobile charge carriers and the resulting electrochemical performance of the fabricated device has not been fully established. Therefore, this study aims to investigate plasticized PLA–$LiClO_4$ polymer electrolytes with varying PC concentrations and to correlate their structural, electrical and electrochemical properties. Fourier-transform infrared spectroscopy (FTIR) is employed to investigate molecular interactions and evaluate the relative contributions of free ions, contact ion pairs and ion aggregates. Ionic conductivity and bulk resistance are determined using AC impedance spectroscopy, while electrochemical impedance spectroscopy (EIS) and linear sweep voltammetry (LSV) are used to assess internal resistance and electrochemical stability. Finally, the capacitive performance of the optimized PLA–$LiClO_4$ based EDLC is evaluated through cyclic voltammetry (CV) and galvanostatic charge–discharge (GCD) measurements, including analyses of specific capacitance, energy density, power density rate capability.

MATERIALS AND METHODS

Materials

Poly(lactic acid) (PLA) with a nominal molecular weight of 116 kg mol^{-1} was purchased from Goodfellow and used as the host polymer. Lithium perchlorate ($LiClO_4$, Acros

Organics, USA) was used as the source of mobile charge carriers. Propylene carbonate (PC) was used as the plasticizer. Dioxane and methanol were used as solvents for dissolving PLA and $LiClO_4$, respectively.

Activated carbon (AC) and carbon black (CB) were used as the active and conductive materials for the electrode fabrication. Poly(vinyl alcohol) (PVA) was used as the polymeric binder. Stainless steel was used as the current collector.

Preparation of plasticized PLA- $LiClO_4$ based polymer electrolyte

The plasticized PLA–$LiClO_4$ polymer electrolytes were prepared using PLA, $LiClO_4$ and PC. Initially, individual PLA solutions were prepared by dissolving 1.00 g of PLA in 10 mL of dioxane. The solutions were stirred for 24 h to ensure complete dissolution of the polymer.

PC was subsequently added to the PLA solutions at concentrations of 10, 30, 50 and 70 wt.%. Each mixture was stirred at 400 rpm and maintained at 60°C for 1 h to obtain homogeneous plasticized PLA solutions. $LiClO_4$ was then added at a fixed concentration of 50 wt.%. Prior to addition, $LiClO_4$ was dissolved in 10 mL of methanol. The resulting mixtures were further stirred at 400 rpm and 60°C for an additional 24 h until homogeneous polymer-electrolyte solutions were obtained. Finally, the prepared solutions were cast into separate Petri dishes and dried at room temperature through slow solvent evaporation to produce free-standing plasticized PLA–$LiClO_4$ polymer-electrolyte films.

Impedance and Conductivity Studies

The thickness of each polymer-electrolyte film was measured using a digital micrometer screw gauge. For impedance measurements, the sample was sandwiched between two stainless-steel blocking electrodes in the configuration:

$$\text{SS | plasticized PLA–LiClO}_4\text{ | SS}$$

The electrochemical impedance measurements were conducted using a ZIVE SP2 impedance potentiostat over a frequency range of 0.1 Hz to 10 kHz at room temperature (27°C). The ionic conductivity of each polymer-electrolyte sample was calculated using Equation 1:

$$\sigma = \frac{l}{R_b A} \tag{1}$$

where σ is the ionic conductivity (S/cm), l is the thickness of sample, R_b is the bulk resistance of sample, which is determined from the Nyquist plot and A is the surface area of the sample.

Linear Sweep Voltammetry Studies

The electrochemical stability of the optimized plasticized PLA–$LiClO_4$ polymer electrolyte was investigated using the linear sweep voltammetry (LSV) technique at room temperature (27 °C). The highest-conductivity polymer electrolyte film was placed between two stainless-steel blocking electrodes in the following configuration:

SS | plasticized PLA–$LiClO_4$ | SS

The potential was swept from -5 to $+5$ Vat a scan rate of 50 mV s^{-1} and the resulting current response was recorded. The cathodic and anodic onset potentials were subsequently determined from the LSV curve using the tangent-line extrapolation method. The electrochemical stability window was then calculated from the difference between the anodic and cathodic onset potentials.

Electrode Preparation

The carbon-based electrodes were prepared by mixing 90 wt.% activated carbon, 5 wt.% carbon black and 5 wt.% PVA binder. The PVA was first dissolved in the selected solvent and stirred until a homogeneous binder solution was obtained. Activated carbon and carbon black were then gradually added to the PVA solution. The mixture was stirred for several hours until a uniform carbon slurry was produced. The prepared slurry was cast onto a stainless steel current collector using the doctor-blade technique. The coated electrodes were dried in an oven at 60°Covernight. Two identical activated-carbon electrodes, each with a geometric area of 2.0 cm^2, were prepared for EDLC fabrication.

EDLC Cell Fabrication

The the optimized plasticized PLA-$LiClO_4$ BPEs was sandwiched between two activated carbon-based electrodes with a surface area of 2.0 cm2, as illustrated in Figure 1. The assembled EDLC cell was subsequently placed in a two-electrode configuration for further electrochemical analysis.

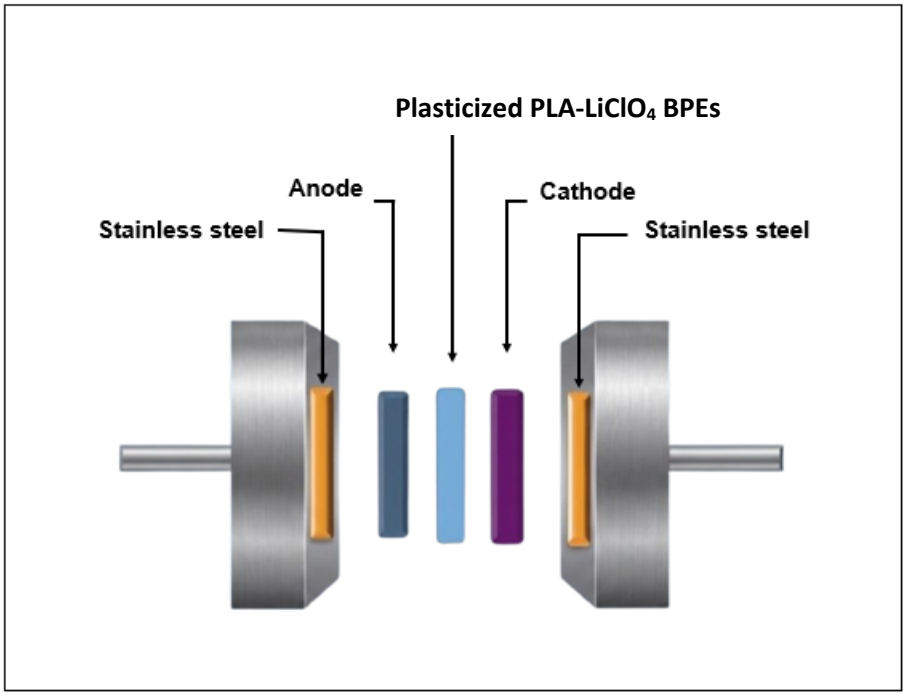

Figure 1. Fabricated EDLC

EDLC Characterization

Cyclic Voltammetry (CV)

CV study to determine the specific capacitance of EDLC. The EDLC cell was then evaluated in a two-electrode system configuration at a scan rate of 1-10 mV/s over a potential range of -1V to 1 V. The specific capacitance (*Csp*) EDLC are computed using the following Equation 2:

$$C_{sp} = \frac{\int_{V_i}^{V_f} I\, dV}{s.m.\Delta V} \tag{2}$$

where is $\int_{V_i}^{V_f} I\, dV$ the integral area under the CV curve, *s* is the potential scan rate (Vs-1), *m* refers to the total mass of electrode active material and ΔV is the potential window [8].

Galvanostatic Charge-Discharge Performance (GCD)

The galvanostatic charge–discharge (GCD) measurements were performed on the fabricated EDLC at current densities of 5, 7 and 10 mA g^{-1} within a potential range of 0–1.0 V. A resting period of 5 s was applied before each charge–discharge cycle. The specific capacitance (C_{sp}, F g^{-1}), energy density (E, Wh kg^{-1}) and power density (P, W kg^{-1}) were calculated using Equations (3), (4)and (5), respectively [9]:

$$C_{sp} = \frac{2I}{m\left(\frac{dV}{dt}\right)} \tag{3}$$

$$E = \frac{C_{sp}\, x\, dV^2}{2}\, x\, \frac{1000}{3600} \tag{4}$$

$$P = \frac{V^2}{4m\, R_{ESR}}, \tag{5}$$

where $R_{ESR} = \frac{\Delta V_{drop}}{2I}$

Results and Discussion

Impedance and Conductivity Analysis

Figures 2 and 3 show the AC conductivity and Nyquist impedance spectra, respectively, of PLA–$LiClO_4$ polymer electrolytes containing different concentrations of PC plasticizer. The AC conductivity values obtained for the 10, 30, 50 and 70 wt.% PC electrolytes were 4.92×10^{-5}, 1.69×10^{-3}, 4.77×10^{-4} and 2.81×10^{-5} S cm^{-1}, respectively. The AC conductivity increased significantly when the PC concentration increased from 10 to 30 wt.%. The conductivity increased from 4.92×10^{-5} S cm^{-1} to 1.69×10^{-3} S cm^{-1}, corresponding to an approximately 34-fold enhancement. This improvement can be attributed to the plasticizing effect of PC. The polar carbonate groups in PC promote the dissociation of $LiClO_4$ into mobile ions, while the increased free volume and flexibility of the PLA matrix enhance polymer-chain segmental motion. These effects improve charge-carrier mobility and facilitate ionic transport through the polymer electrolyte [10]. The maximum conductivity observed at 30 wt.% PC indicates that this composition

provides the optimum balance between mobile charge-carrier concentration and ionic mobility. However, further increasing the PC concentration resulted in a reduction in conductivity. The conductivity decreased to 4.77×10^{-4} S cm^{-1} at 50 wt.% PC and further decreased to 2.81×10^{-5} S cm^{-1} at 70 wt.% PC. Compared with the 30 wt.% PC electrolyte, these values correspond to decreases of approximately 71.8% and 98.3%, respectively. The decrease at high PC concentrations may be associated with excessive plasticization and dilution of the $LiClO_4$ concentration. Although PC increases polymer-chain flexibility, an excessive amount may reduce the effective concentration of mobile charge carriers and disrupt the continuous PLA-based ion-transport network. Ion aggregation, reduced polymer–salt interactions, or phase separation may also contribute to the reduction in conductivity [11]. These mechanisms should be further verified using complementary characterization techniques such as FTIR.

The Nyquist plots show mainly inclined low-frequency responses without clearly resolved semicircles. This behavior is associated with ionic transport and electrode polarization at the electrolyte–electrode interface. The 30 wt.% PC sample is located closest to the origin, indicating the lowest apparent impedance and the lowest resistance among the investigated compositions. The 50 wt.% PC sample exhibits an intermediate impedance response, while the 10 and 70 wt.% PC samples are shifted towards higher (Z') values. The 70 wt.% PC electrolyte displays the largest impedance response, indicating the greatest resistance to ion transport. In addition to the position of the spectra, the gradient of the low-frequency response also provides information about the electrochemical behavior of the electrolytes [12]. The 30 wt.% PC spectrum exhibits the steepest and most nearly vertical response among the samples. This indicates a stronger capacitive contribution and more pronounced electrode polarization, suggesting that ions can accumulate more effectively at the electrode–electrolyte interface. This observation is consistent with the high ionic conductivity and low impedance of the 30 wt.% PC electrolyte. The 50 wt.% PC spectrum shows an intermediate gradient, whereas the 10 and 70 wt.% PC spectra display comparatively more inclined responses. These less-steep gradients indicate a greater contribution from resistive or diffusion-related processes and less ideal capacitive behavior [13].

For an ideal EDLC, the low-frequency region of the Nyquist plot would approach a vertical line, corresponding to ideal capacitive behavior [14]. The inclined profiles observed in this study indicate that the electrolytes exhibit non-ideal capacitive behavior due to finite ionic diffusion, electrolyte resistance and interfacial polarization. However, the gradient should be interpreted qualitatively because an accurate separation of bulk resistance, charge-transfer resistance and constant-phase-element behavior requires equivalent-circuit fitting. Therefore, the lower impedance and steeper capacitive response of the 30 wt.% PC sample correspond to its higher ionic conductivity. Conversely, the high impedance and less ideal gradient of the 70 wt.% PC sample correspond to its low conductivity and poorer ion-transport capability.

Overall, both the AC conductivity and impedance results demonstrate that PC concentration strongly influences the ionic transport and capacitive behavior of PLA–$LiClO_4$ polymer electrolytes. The 30 wt.% PC electrolyte exhibits the highest conductivity of 1.69×10^{-3} S cm^{-1}, the lowest apparent impedance and the most pronounced capacitive gradient. Therefore, the 30 wt.% PC composition is the most promising electrolyte for further EDLC applications because its high ionic conductivity

and favorable impedance response can reduce internal resistance, improve ion transport and enhance charge–discharge performance. Further confirmation should be obtained through equivalent-circuit fitting, galvanostatic charge–discharge testing, cycling stability evaluation and complete EDLC-cell impedance measurements.

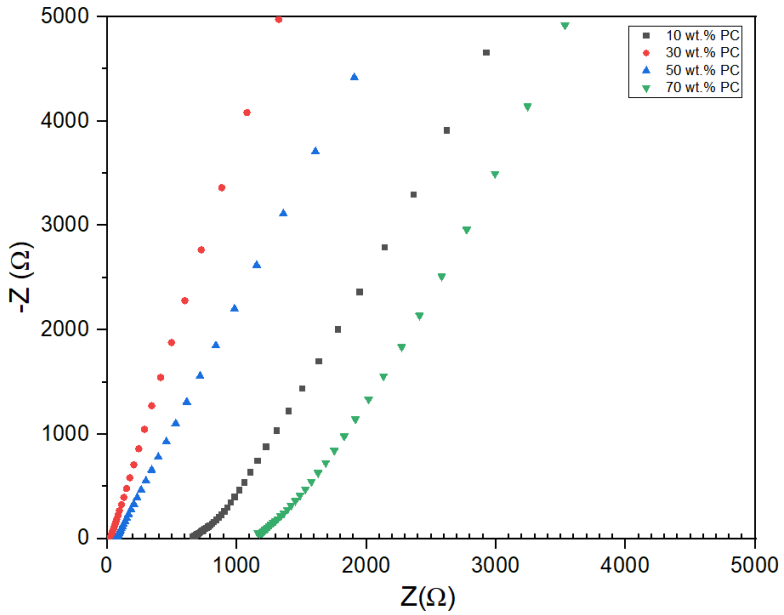

Figure 2. Nquist plot of different concentration of Propylene Carbonate in PLA–$LiClO_4$ SPEs

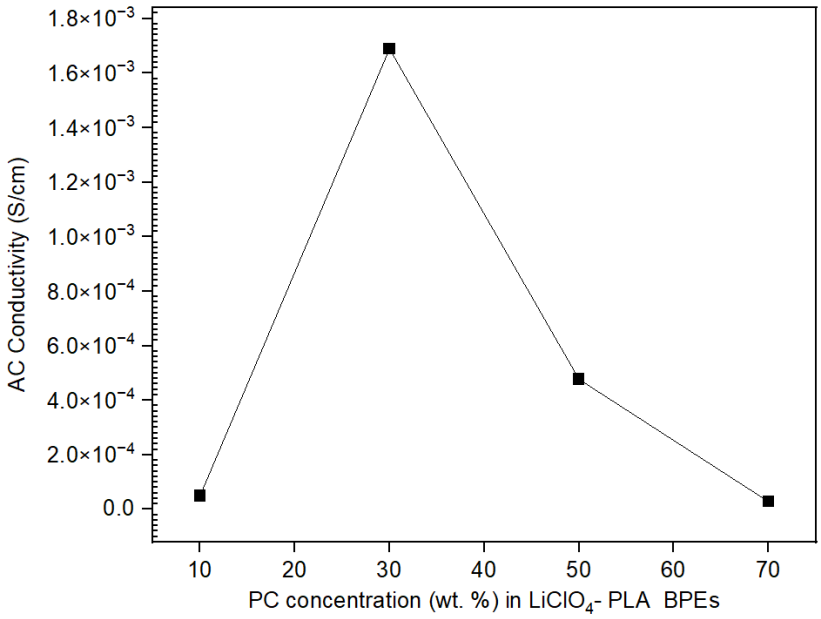

Figure 3 Conductivity of different concentration of Propylene Carbonate in PLA–$LiClO_4$ SPEs

ATR-FTIR Analysis

The effect of PC concentration on the structural, ionic and electrical properties of PLA–$LiClO_4$ polymer electrolytes was investigated using FTIR spectroscopy, spectral deconvolution, electrochemical impedance spectroscopy and AC conductivity analysis. The corresponding FTIR spectra and deconvoluted ionic-species profiles are presented in Figures 4 and 5.

Figure 4 shows the FTIR spectra of PLA–$LiClO_4$ polymer electrolytes containing 10, 30, 50 and 70 wt.% PC. The spectra were vertically offset for clarity. The main absorption band at approximately 1754 cm^{-1} is attributed mainly to the ester carbonyl (C=O) stretching vibration of PLA, with possible overlapping contributions from the carbonate carbonyl group of PC [15, 16]. Other bands observed at approximately 1452-1456 cm^{-1}, 1359-1360 cm^{-1}, 1208-1213 cm^{-1}, 1179-1181 cm^{-1}, 1126-1128 cm^{-1}, 1082-1083 cm^{-1} and 1044-1046 cm^{-1} are associated mainly with CH_3 deformation, C–O–C stretching and perchlorate-related vibrations [17].

The carbonyl absorption in the 1650–1800 cm^{-1} region becomes progressively stronger from 10 to 50 wt.% PC. Since the spectra are plotted in percentage transmittance, stronger absorption appears as a deeper band and a lower transmittance value. This increase in intensity is mainly caused by the increasing amount of PC, which introduces additional carbonate carbonyl groups into the PLA–$LiClO_4$ matrix. The carbonyl oxygen atoms can also coordinate with Li^+ ions, modifying the local dipole environment and contributing to changes in the intensity and width of the carbonyl band [18]. The strongest relative carbonyl absorption is observed at 50 wt.% PC, indicating a greater contribution from PC carbonate groups and stronger interactions between PC, PLA and $LiClO_4$.

However, the increase in carbonyl intensity does not directly indicate higher ionic conductivity. The FTIR intensity reflects the number and chemical environment of the carbonyl groups, whereas conductivity depends on both the number of mobile ions and their mobility. The 70 wt.% PC spectrum shows a less pronounced carbonyl absorption than the 50 wt.% PC spectra. This apparent reduction indicates structural heterogeneity or phase separation caused by excessive plasticization [19]. The main carbonyl band remains at approximately 1754 cm^{-1} for all compositions, indicating that the PLA ester structure is retained and that PC mainly acts through plasticization and Li^+ coordination rather than forming a new covalent structure.

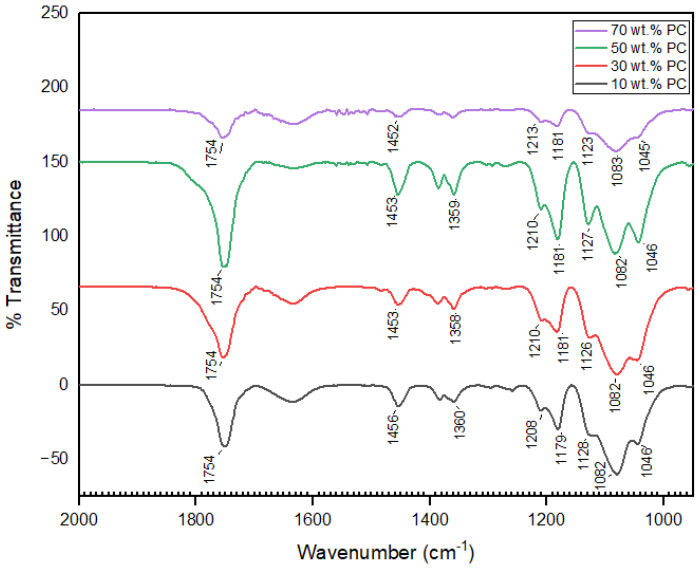

Figure 4. FTIR spectra of PLA–$LiClO_4$ polymer electrolytes containing 10, 30, 50 and 70 wt.% PC

The ionic species were further analyzed by deconvoluting the perchlorate-related absorption region, as shown in Figure 5(a–d). The fitted components were assigned to free ions, contact ion pairs and ion aggregates. The percentages obtained from the deconvolution and the corresponding AC-conductivity values are summarized in Table 1.

Table 1. The aggregation, contact and free ions percentage obtained from the deconvolution and the corresponding AC-conductivity values of different concentration of PC in $LiClO_4$-PLA BPEs

PC concentration	Ion aggregates (%)	Contact ions (%)	Free ions (%)	AC conductivity (S cm^{-1})
10 wt.%	21.40	22.44	56.16	4.92×10^{-5}
30 wt.%	18.48	15.81	65.71	1.69×10^{-3}
50 wt.%	29.79	27.05	43.15	4.77×10^{-4}
70 wt.%	26.30	18.36	55.34	2.81×10^{-5}

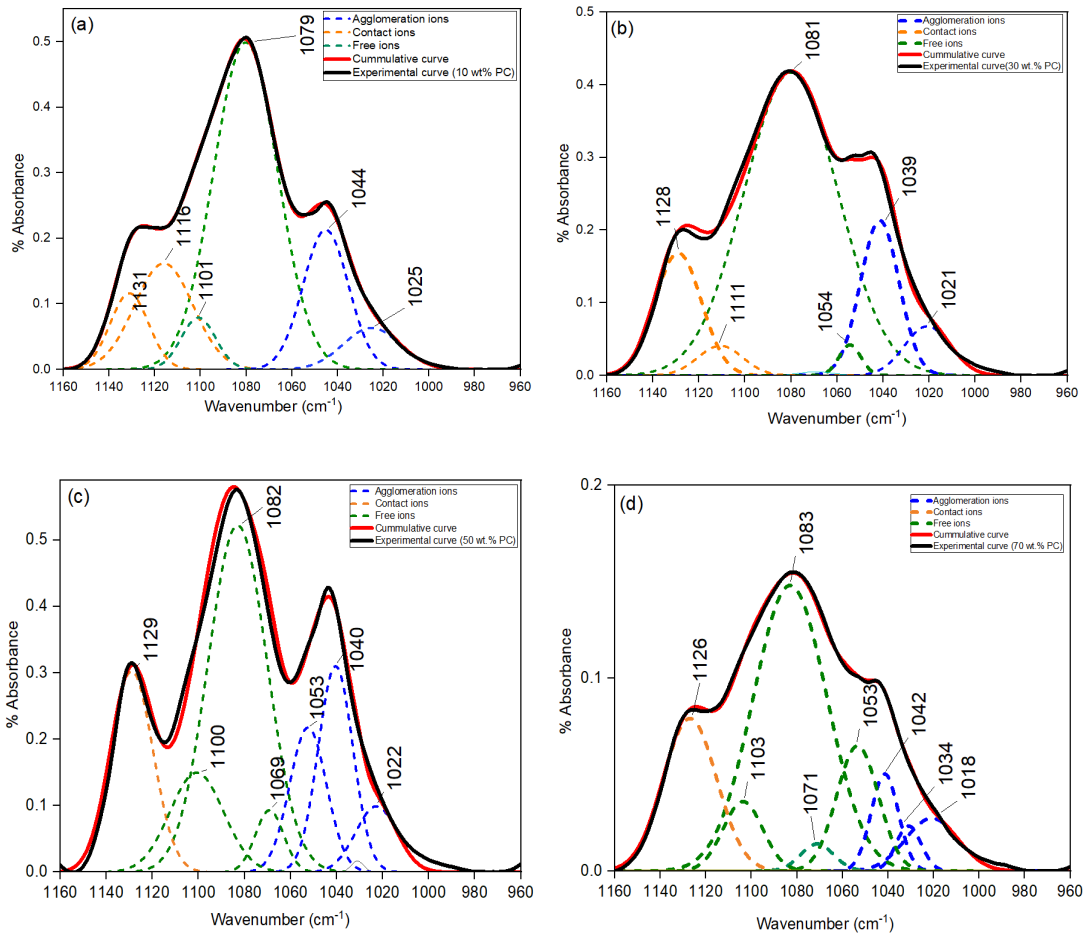

Figure 5. Deconvolution of the perchlorate-related absorption band for (a) 10 wt.% PC, (b) 30 wt.% PC, (c) 50 wt.% PC and (d) 70 wt.% PC. The dashed curves represent free ions, contact ion pairs and ion aggregates, while the red and black curves represent the cumulative and experimental spectra, respectively

At 10 wt.% PC, the free-ion fraction was 56.16%, while the contact-ion-pair and aggregate fractions were 22.44% and 21.40%, respectively. The conductivity was relatively low at 4.92×10^{-5}S cm^{-1}. Although free ions were the dominant species, the low PC content was insufficient to provide effective plasticization of the PLA matrix. Consequently, the polymer chains remained relatively rigid, limiting segmental motion and restricting the mobility of the available ions [20].

The increase in PC concentration to 30 wt.% resulted in an increase in the free-ion fraction to 65.71%. At the same time, the fractions of contact ion pairs and aggregates decreased to 15.81% and 18.48%, respectively. This indicates that 30 wt.% PC promoted $LiClO_4$ dissociation and reduced ion association. The polar carbonate groups of PC can interact with Li^+ ions, while the increased free volume and flexibility of the PLA matrix facilitate ion movement[21]. As a result, the conductivity increased significantly to 1.69×10^{-3}S cm^{-1}, which was approximately 34 times higher than that of the 10 wt.%

PC sample. The 30 wt.% PC composition therefore provided the most favourable balance between free-ion formation and ionic mobility.

The decrease in ionic conductivity at 50 wt.% PC is consistent with previous findings by Brooks and Fawcett reported that the ionic conductivity of $LiClO_4$–PEO electrolytes initially increased with increasing propylene carbonate content due to the higher concentration of free ions. However, further addition of PC promoted the formation of contact ion pairs and ion aggregates, resulting in a decrease in ionic conductivity. A similar trend was observed in the present PLA–$LiClO_4$ system, where excessive PC likely enhanced Li^+–carbonyl interactions, increasing ion association and reducing the concentration of free ions available for ionic transport [17].

At 70 wt.% PC, the free-ion fraction increased again to 55.34%, while the contact-ion-pair fraction decreased to 18.36%. However, the ion-aggregate fraction remained relatively high at 26.30%. Despite the partial increase in free ions, the conductivity decreased drastically to 2.81×10^{-5} S cm^{-1}. This result demonstrates that the free-ion fraction alone cannot determine the conductivity of the polymer electrolyte. Excessive PC may cause over-plasticization, disrupt the continuous PLA polymer structure and create heterogeneous ion-transport regions. Consequently, some ions identified as free by spectral analysis may not contribute effectively to long-range ionic conduction.

Overall, the results demonstrate that ionic conductivity is governed by the combined effects of ion dissociation, ion association and polymer-chain mobility. The increase in free ions and decrease in contact ion pairs and aggregates from 10 to 30 wt.% PC corresponded to a substantial increase in conductivity. In contrast, the decrease in free ions and increase in associated species at 50 wt.% PC resulted in lower conductivity. Although the free-ion fraction increased again at 70 wt.% PC, the high aggregate content and possible structural disruption caused the conductivity to decrease further. Therefore, 30 wt.% PC was identified as the optimum composition, providing the highest free-ion fraction, the lowest degree of ion association and the highest AC conductivity.

Linear Sweep Voltammetry (LSV) Analysis

Figure 6 shows the LSV profile of the EDLC device measured over a potential range of −5 to +5 V. The current density increased in the cathodic direction at potentials below approximately −2.8 V, reaching about -2.8×10^{-3} A g^{-1} at −5 V. This increase suggests the onset of a reduction process or possible electrolyte decomposition at highly negative potentials.

Within the potential range of approximately −2.8 to +2.8 V, the current density remained relatively low and close to the baseline. No distinct oxidation or reduction peaks were observed in this region, indicating the absence of significant faradaic reactions. This behavior is consistent with predominantly non-faradaic charge storage through the electrostatic accumulation of ions at the electrode–electrolyte interface, as expected for an EDLC.

At positive potentials above approximately +2.8 V, the anodic current increased rapidly and reached about 3.2×10^{-3} A g^{-1} at +5 V. The anodic onset potential was determined to be +2.8 V using the tangent-line extrapolation method. Similarly, the cathodic onset potential was estimated to be −2.8 V. Therefore, the apparent electrochemical stability window was calculated using Equation 6:

$$\Delta E = E_{\text{anodic}} - E_{\text{cathodic}} \quad (6(a))$$

$$\Delta E = (+2.8) - (-2.8) = 5.6\ \text{V} \quad (6(b))$$

The resulting apparent stability window of 5.6 V is relatively broad compared with several recently reported plasticized biopolymer electrolytes. A plasticized sodium carboxymethyl cellulose/pectin/lithium perchlorate (NaCMC/pectin/$LiClO_4$) electrolyte was reported to remain electrochemically stable up to approximately 3.3 V [22], while a plasticized NaCMC/PEO/$LiClO_4$ electrolyte exhibited a stability window of approximately 3.2 V [23]. The 5.6 V window obtained in the present study is therefore approximately 70–75% wider than these reported values. A fish-gelatin/$LiClO_4$ biopolymer electrolyte reported an electrochemical stability window of approximately 1.88 V [7], indicating that the present PLA–$LiClO_4$ system also provides a broader apparent stability range than that earlier biodegradable electrolyte.

A related plasticized PLA-based electrolyte containing Lithium trifluoromethanesulfonate ($LiCF_3SO_3$) and carbonate plasticizer was reported to exhibit an LSV potential window of approximately 7.10 V [24]. Although this value is higher than the 5.6 V obtained in the present study, the comparison should be treated cautiously because the reported system used a different lithium salt, plasticizer composition, electrolyte formulation, electrode configuration and onset-current criterion. The present result is therefore best interpreted as evidence of a comparatively wide electrochemical stability window for the PLA–$LiClO_4$ formulation rather than as a direct ranking against all other polymer electrolytes.

The sharp current increase beyond ±2.8 V indicates that the applied potential has exceeded the stability limit of the electrolyte/electrode system. At the positive limit, oxidation of the polymer, plasticizer, anion, or electrode surface may occur, whereas reduction processes may occur at the negative limit. These side reactions can cause gas formation, increased leakage current, electrode degradation, chemical changes in the electrolyte and accelerated loss of capacitance during long-term cycling. The relatively low current response within the −2.8 to +2.8 V region indicates that these degradation reactions remain limited within the apparent stable region.

Overall, the LSV profile demonstrates that the PLA–$LiClO_4$ electrolyte exhibits a broad apparent electrochemical stability window of approximately 5.6 V, with no clear faradaic peaks within the central stable region. This result compares favorably with recent $LiClO_4$-based plasticized biopolymer electrolytes, which generally report stability windows of approximately 3.2–3.3 V. The wide stability range, together with the high ionic conductivity observed for the optimized 30 wt.% PC composition, supports the potential use of this electrolyte in EDLC applications. Nevertheless, the practical voltage window should be confirmed using complete two-electrode EDLC cells through CV, GCD, EIS, leakage-current testing, IR-drop analysis and long-term cycling.

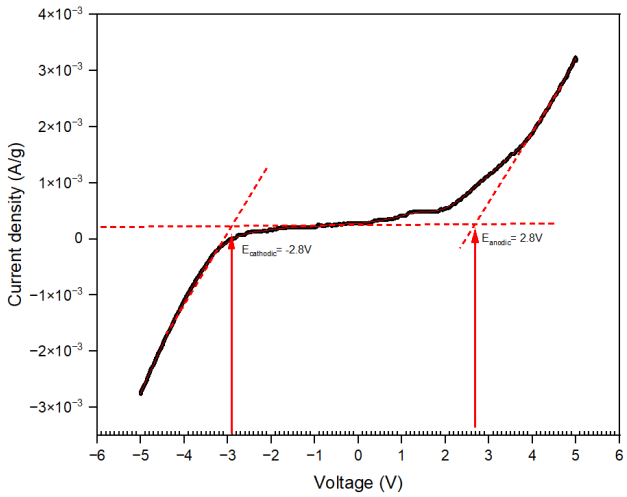

Figure 6. The LSV curve for optimal concentration PC wt.% in samples

Cyclic Voltammetry Analysis

The electrochemical performance of the developed plasticized PLA–$LiClO_4$ based EDLC was characterized using Cyclic Voltammetry (CV) within a potential window of -1.0 V to 1.0 V at various scan rates ranging from 1 mV s^{-1} to 10 mV s^{-1} as shown in Figure 7. Ideally, a perfect EDLC exhibits a highly symmetrical rectangular CV curve, reflecting instantaneous double-layer charging via pure electrostatic ion accumulation at the electrode-electrolyte interface. However, the CV curves obtained for this system deviate from the ideal rectangular shape, displaying an elongated, tilted leaf-like (or quasi-rectangular) geometry. The absence of distinct oxidation and reduction peaks across all scan rates confirms that the charge storage mechanism is predominantly capacitive (EDLC behavior) through non-faradaic processes rather than pseudocapacitive faradaic redox reactions [25]. Meanwhile, the noticeable tilting of the CV loops signifies the presence of internal ohmic resistance, also known as Equivalent Series Resistance (ESR), within the EDLC system. This resistance likely originates from the bulk resistance of the plasticized PLA electrolyte, the interfacial resistance between the polymer electrolyte and the electrodes, or the intrinsic electronic resistance of the current collectors.

As the scan rate increases from 1 mV s^{-1} to 10 mV s^{-1}, several key kinetic and diffusion trends become apparent, leading to a significant dependency of the specific capacitance on the operational speed. The current response scales up proportionally with the scan rate, causing the area under the CV curve to increase at higher rates like 7 mV s^{-1} and 10 mV s^{-1}. This is a standard kinetic characteristic of electrochemical capacitors, where faster potential changes force rapid charge movement. Consequently, the calculated specific capacitance shows a prominent downward trend as the scan rate accelerates. The cell delivers its maximum specific capacitance of 47.43 F g^{-1} at a lower scan rate of 1 mV s^{-1}. As the scan rate increases to 3 mV s^{-1} and 5 mV s^{-1}, the specific capacitance drops sharply to 15.82 F g^{-1} and 6.91 F g^{-1}, before further tailing off to 4.71 F g^{-1} at 7 mV s^{-1} and reaching its minimum value of 3.25 F g^{-1} at 10 mV s^{-1}.

This inverse relationship between specific capacitance and scan rate is closely tied to diffusion limitations within the matrix. At higher scan rates (e.g., 10 mV s^{-1}), the Li^+ and ClO_4^- ions within the plasticized PLA matrix have insufficient time to diffuse into the

deeper, inner pores of the electrodes and fully organize at the interface, thereby restricting charge storage to only the outermost surface of the electrodes. A similar trend was reported in a comparative study by Kar Kien Ong et al. utilizing a hydrogel polymer electrolyte (HPE) synthesized via glutaraldehyde-induced chemical crosslinking of poly(vinyl alcohol) (PVA), sulfuric acid (H_2SO_4) and lithium triflate (LiOTf). In their work, the reduction in capacitance at higher scan rates was strongly attributed to the steric hindrance of the bulky triflate anions ($CF_3SO_3^-$), which lack sufficient time to penetrate deeply into the micropores of the activated carbon electrodes under accelerated operational speeds, thereby limiting charge storage [8].

Furthermore, this behavior aligns closely with another investigation by Kar Kien Ong et al. (2026) on a / lithium bis(tri-fluoromethanesulfonyl) imide(LiTFSI)/1-butyl-3-methylimidazolium bis(trifluoromethylsulfonyl) imide (BmimTFSI)-functionalized poly(acrylic acid)-based ionogel polymer electrolyte (designated as TF35). Their TF35 ionogel EDLC manifested specific capacitances of 67, 61, 56, 52 and 50 F g^{-1} at scan rates of 10, 15, 20, 25 and 30 mV s^{-1}, respectively. They similarly concluded that high CV scan rates induce a reduction in capacitance due to the rapid consumption of ions at the immediate surface of the carbon electrode. This leaves insufficient time for the ions to penetrate deeply into the bulk of the carbon electrode structure, resulting in limited charge storage [26].

Comparatively, both the TF35 ionogel and the plasticized PLA- $LiClO_4$ system operate within similar low millivolt scan rate windows, demonstrating the classic diffusion-controlled kinetics of solid/gel polymer matrices. Although the perchlorate (ClO_4^-) anions in this PLA system are smaller than both triflate and TFSI anions, they face a comparable diffusion bottleneck as the scan rate scales up from 1 to 10 mV s^{-1} due to the dense, macromolecular nature of the solid-like PLA host. This diffusion constraint increases the effective internal resistance of the cell, visibly manifesting as a more severe tilt in the 10 mV s^{-1} CV loop. Conversely, at lower scan rates, the ions have ample time to overcome these spatial constraints, allowing them to migrate and thoroughly penetrate the porous structure of the electrodes to yield a substantially higher capacitance.

This overall electrochemical behavior is fundamentally governed by the macromolecular nature of the plasticized PLA + $LiClO_4$ polymer electrolyte matrix. The incorporation of a plasticizer into the PLA matrix is crucial because it disrupts the crystalline regions of the polymer, increases the free volume and enhances polymer chain flexibility. This structural modification facilitates smoother segmental motion, allowing the dissociated Li^+ and ClO_4^- ions to migrate more freely under the applied electric field. Nevertheless, the rapid drop in specific capacitance from 47.43 F g^{-1} to 3.25 F g^{-1} highlights the typical ionic conductivity limitations inherent to solid-like polymer matrices when compared to low-viscosity liquid or highly porous crosslinked hydrogel systems under high-speed operational demands.

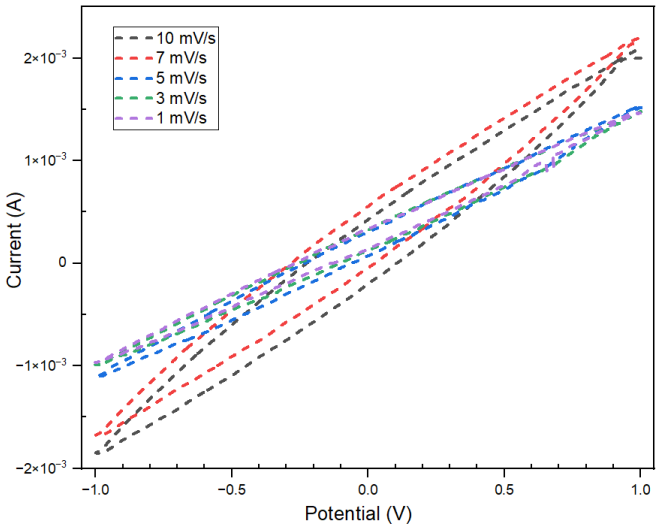

Figure 7. Cyclic Voltammetry (CV) plotted of the fabricated EDLC at various scan rate

Galvanostatic Charge- Discharge Analysis

The capacitive capability and rate performance of the developed plasticized PLA-$LiClO_4$ based EDLC were further evaluated using Galvanostatic Charge-Discharge (GCD) measurements within a potential window of 0.0 V to 1.0 V. As shown in Figure 8, the GCD profiles were recorded at three distinct current densities: 5 mA g^{-1}, 7 mA g^{-1} and 10 mA g^{-1}. Ideally, a perfect EDLC exhibits highly symmetrical and linear triangular profiles, signifying excellent capacitive behavior and highly reversible electrostatic ion accumulation at the electrode-electrolyte interface. For this developed system, the GCD curves display a quasi-triangular shape with slight non-linearity during the charging and discharging segments. This deviation from perfect linearity indicates a transition from pure electrostatic double-layer capacitance to slightly diffusion-controlled kinetics, which is highly typical for solid or gel-like polymer electrolyte matrices where ion transport is slower compared to liquid electrolytes.

A critical observation from the GCD profiles is the change in discharge time (Δt) as a function of current density, which directly influences the calculated specific capacitance (C_sp). At the lowest current density of 5 mA g^{-1}, the cell exhibits the longest discharge time, extending to 2209.95 s. This prolonged duration allows the dissociated Li^+ and ClO_4^- ions within the plasticized PLA host sufficient time to migrate, overcome steric barriers and penetrate the deeper micropores of the activated carbon electrodes, yielding a maximum specific capacitance of 22.44 F g^{-1}. Conversely, as the current density increases to 7 mA g^{-1} and 10 mA g^{-1}, the discharge durations decrease drastically to 925.76 s and 398.82 s, respectively, resulting in lower specific capacitance values of 13.35 F g^{-1} and 9.62 F g^{-1}. Under these accelerated conditions, ions are rapidly driven toward the electrode surface, leading to shallow charge accumulation confined mainly to the outermost electrode interface due to insufficient time for deep pore diffusion.

Additionally, the GCD curves exhibit a noticeable voltage drop, known as the IR drop, at the beginning of the discharge cycle. This sudden, sharp vertical drop in voltage is a direct

manifestation of the internal resistance of the system, commonly referred to as the equivalent series resistance (ESR). At a low current density of 5 mA g^{-1}, the cell registers a minimal IR drop of 0.0144 V. However, as the current density increases to 7 mA g^{-1} and 10 mA g^{-1}, the IR drop increases significantly to 0.0270 V and 0.1696 V, respectively. This increasing trend occurs because higher current loads amplify the internal ohmic drop across the bulk electrolyte and interfaces. The presence of this IR drop correlates well with the previous cyclic voltammetry (CV) findings, where a tilted, leaf-like loop geometry was observed at higher scan rates.

The energy density (E, in Wh kg^{-1}) and power density (P, in W kg^{-1}) of the fabricated EDLC device were evaluated based on the discharge profiles to determine its practical performance. At a current density of 5 mA g^{-1}, the device delivers its highest energy density of 3.12 Wh kg^{-1} with a corresponding power density of 173.61 W kg^{-1}. As the current density increases to 7 mA g^{-1}, the energy density decreases to 1.85 Wh kg^{-1}, while the power density decreases to 129.63 W kg^{-1}. Upon reaching the highest applied current density of 10 mA g^{-1}, the device maintains an energy density of 1.34 Wh kg^{-1} but experiences a significant reduction in power density to 29.48 W kg^{-1}. This simultaneous decrease in performance parameters at higher current loads is a direct consequence of the increased IR drop (0.1696 V) and severe ion-transport limitations under rapid charging and discharging conditions. In summary, while the plasticized PLA electrolyte successfully facilitates ion transport through enhanced polymer segmental motion, the rate-dependent reduction in performance parameters highlights the mass-transport and diffusion limitations inherent to macromolecular polymer structures under high current demands.

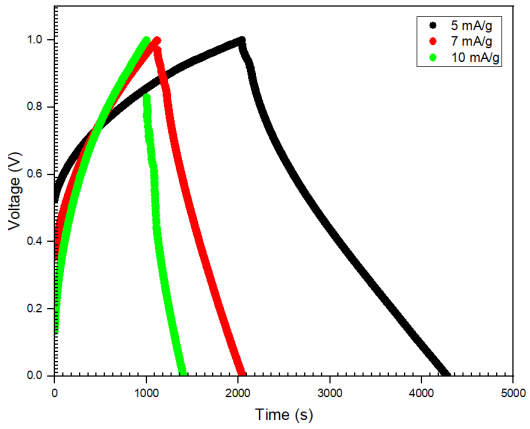

Figure 8. The GCD curves with variation of current density of fabricated EDLC

CONCLUSIONS

Plasticized PLA–$LiClO_4$ polymer electrolytes were successfully prepared and investigated as biodegradable solid polymer electrolytes for electric double-layer capacitor (EDLC) applications. The incorporation of propylene carbonate (PC) was found to play an important role in improving the electrolyte properties, particularly by enhancing ion dissociation, polymer-chain flexibility and ion mobility. Among the compositions studied, the electrolyte containing 30 wt.% PC exhibited the best overall

performance, achieving the highest ionic conductivity of 1.69×10^{-3} S cm^{-1}, lower impedance and improved ion transport behavior due to the balanced interactions between the PLA matrix, $LiClO_4$ salt and plasticizer.

The optimized electrolyte demonstrated good electrochemical stability, with a wide stability window of approximately 5.6 V. The absence of significant redox peaks in the cyclic voltammetry (CV) analysis confirmed that the fabricated EDLC stored energy mainly through an electric double-layer charge storage mechanism. The device achieved a maximum specific capacitance of 47.43 F g^{-1} at 1 mV s^{-1}, while galvanostatic charge–discharge (GCD) measurements showed the highest specific capacitance of 22.44 F g^{-1} at 5 mA g^{-1}, supported by a long discharge time of 2209.95 s. These results indicate that sufficient time for ion migration enables effective charge accumulation within the porous activated-carbon electrodes.

However, increasing the current density resulted in reduced capacitance, shorter discharge time and a larger IR drop, indicating limitations associated with ion diffusion and internal resistance during rapid charge–discharge processes. The EDLC achieved a maximum energy density of 3.12 Wh kg^{-1} and power density of 173.61 W kg^{-1} at 5 mA g^{-1}, demonstrating the capability of the PLA–$LiClO_4$ electrolyte for low-to-moderate-rate energy storage applications. Overall, the 30 wt.% PC plasticized PLA–$LiClO_4$ electrolyte provides a promising balance between ionic conductivity, stability and capacitive performance. Further improvements in electrolyte formulation, electrode–electrolyte interfaces, pore structure optimization and long-term cycling stability are required to enhance the rate capability and support future practical applications of biodegradable polymer electrolyte-based EDLC systems.

ACKNOWLEDGEMENTS

The author acknowledges Universiti Teknologi MARA (UiTM) Pahang for providing the facilities and support for this research.

AUTHORS' CONTRIBUTIONS STATEMENT

Fairuzdzah Ahmad Lothfy conceptualized and led the project, designed the study, supervised the research activities, and contributed to the writing, review, and editing of the manuscript. Nur Ainul Mardhiyah Shahri Zaili contributed to sample preparation and experimental measurements. Nurul Infaza Talalah Ramli and Siti Zafirah Zainal Abidin contributed to the preparation, review, and editing of the manuscript. All authors contributed to the discussion of the results, reviewed the manuscript, and approved the final version of the manuscript.

COMPETING INTERESTS

The authors declare that they have no relevant financial or non-financial interests

DATA AVAILABILITY

The datasets used and/or analyzed during the current study are available from the corresponding author upon reasonable request.

REFERENCES

[1] International Energy Agency, Batteries and Secure Energy Transitions: Executive summary. 2025. [Online]. Available: https://www.iea.org/reports/batteries-and-secure-energy-transitions/executive-summary.

[2] Elashnikov R, Khrystonko O, Jilková T, Rimpelová S, Prchal J, Ivan Khalakhan, Zdeňka Kolská, Václav Švorčík, Oleksiy Lyutakov et al., High-strength self-healable supercapacitor based on supramolecular polymer hydrogel with upper critical solubility temperature. *Advances in Functional Materials*. 2024;34(23):1–11.

[3] Nandhinilakshmi M, Vanitha D, Nallamuthu N, Sundaramahalingam K, Saranya P, Shameem Abdul Samad. High performance lithium ion-conducting plasticized biopolymer electrolyte for supercapacitor application. *Journal of Polymers and the Environment.* 2024;32:5157–5178.

[4] Abdulwahid RT, Aziz SB, Kadir MFZ. Replacing synthetic polymer electrolytes in energy storage with flexible biodegradable alternatives: sustainable green biopolymer blend electrolyte for supercapacitor device. *Materials Today Sustainability.* 2023;23:1-17.

[5] Sadiq NM, Abdulwahid RT, Mohammed PA, Aziz SB, Woo HJ, Kadir MFZ. Advancements in green polymer blend nanocomposite electrolytes (PPBNEs) and activated carbon for EDLC application with high energy density. *Journal of Energy Storage*. 2024; 93;112282 .

[6] Ahmad Lothfy F, Ali AMM, Ahmad Rafaie H, Hassan MS, Zainal Abidin SZ, Conductivity and dielectric study of polylactic acid- lithium perchlorate solid polymer electrolyte film. *Defect and Diffusion Forum*. 2022;(421):99–109.

[7] Kadir MFZ. Non-Faradaic-based supercapacitor fabricated with fish skin gelatin biopolymer electrolyte. *Ionics (Kiel).* 2021;27(5):1–11.

[8] Ong KK, Heng SF, Choy CW, Liew CW. Glutaraldehyde-crosslinked poly (vinyl alcohol) hydrogel polymer electrolytes for Electrical Double Layer Capacitor (EDLC) Applications. *Journal of Physics and Chemistry of Solids.* 2026; 17:1-13.

[9] Jacky Y, Winie T, Ho WL, Khandaker MU, Purwanto A, Aziz SB, Sangaraju S, Woo HJ. Enhanced energy density in electric double layer capacitors using metal-organic framework as filler in biodegradable poly(vinyl) alcohol-based solid-state electrolytes. *Journal of Energy Storage*. 2026;141:1-21.

[10] Aziz SB, Aziz DM, Hama PO, Abdulwahid RT, Sadiq NM, Al-Saeedi SI, Kadir MFZ, Sangaraju S, Yong J, Woo HJ. Unlocking high energy density and stable electric double layer capacitor derived from sustainable biodegradable polymer electrolyte based on chitosan:polyvinyl alcohol: Potassium thiocyanate:xGlycerol ($10 \leq x \leq 30$). *Results in Engineering.* 2025;27;106897.

[11] Bushkova O. V, Erkabaev AM, Yaroslavtseva TV, Reznitskikh OG. Ion aggregation and phase separation in amorphous poly(nitrile)-based lithium conducting polymer electrolytes. *Solid State Ionics*. 2019;333:57–65.

[12] Lazanas AC, Prodromidis MI. Electrochemical impedance spectroscopy─A tutorial. *ACS Measurement Science Au.* 2023; 3(3):162–193.

[13] Bel E, Jrad H, Soavi F. Development and performances analysis of eco- friendly pullulan/polyvinyl alcohol composites based all-solid-state supercapacitors. *Journal of Materials Chemistry A*. 2026;14(20):12025–12035.

[14] Mei BA, Munteshari O, Lau J, Dunn B, Pilon L. Physical interpretations of Nyquist plots for EDLC electrodes and devices. *The Journal of Physical Chemistry C*. 2018;122(1): 194–206.
[15] Mohtar LG, Ledesma AE, Disalvo EA, Frias MA. Influence of carbonyl groups on the interaction of PLA_2 with lipid interphases. *Colloid and Interface Science Communications.* 2020;9:100309
[16] Clark JB, Allen HC. Interfacial carbonyl groups of propylene carbonate facilitate the reversible binding of nitrogen dioxide. *Physical Chemistry Chemical Physics.* 2024;26(21):15733–15741.
[17] Ahmed HT, Abdullah OG. Structural and ionic conductivity characterization of PEO:MC-NH_4I proton-conducting polymer blend electrolytes based films. *Results in Physics.* 2020;16:102861.
[18] Zhang B, Zhou Y, Li X, Ren X, Nian H, Shen Y, Yun Q. Ion-molecule Interaction in solutions of lithium tetrafluoroborate in propylene carbonate: An FTIR vibrational spectroscopic study. *International Journal of Electrochemical Science.* 2013;8(12):12735–12740.
[19] Caroline R Szczepanskia, Carmem S Pfeiferb, Jeffrey W S. A new approach to network heterogeneity: Polymerization Induced Phase Separation in photo-initiated, free-radical methacrylic systems Caroline, *NIH Public Access*, 2012;53(21):4694–4701.
[20] Jefri ES, Mohd Hanafi MH, Razak NH, Abdul Manaf MZ, Md Yusof FA, Suhaimy SHM and Grasianto. A study review on mechanical properties of polylactic acid (PLA) with plasticizer vegetable based and composite material. *Chemical Engineering Transactions.* 2025;122:415–420.
[21] Liu Y, Zeng O, Li Z, Chen A, Guan J, Wang H, Wang S, Zhang L. Recent development in topological polymer electrolytes for rechargeable lithium batteries. *Advanced Science.* 2023;10(15):1–29.
[22] Khellouf RA, Bubulinca C, Cyriac V, Cisar J, Durpekova S, Sedlarik V. Insight into structure-property correlations in plasticized sodium carboxymethyl cellulose/pectin blend-based polymer electrolyte for EDLC application. *Journal of Energy Storage*. 2024;101:113769.
[23] Khellouf RA, Cyriac V, Bubulinca C, Sedlarik V. Deciphering the role of $LiClO_4$ salt on electrochemical properties of plasticized biopolymer electrolytes for superior EDLC efficiency at elevated temperatures. *Energy & Environmental Materials*. 2025;8(5):1–11.
[24] Ahmad Lothfy F, Ali AMM, Zainal Abidin SZ. Plasticized lithium ion conducting PLA based polymer electrolyte for application in EDLC. *Journal of Advanced Research in Fluid Mechanics and Thermal Sciences.* 2025;128(2):1–13.
[25] Akabbouch L, Khoujaa OE, Assahsahic I, Dassallema S, Ait-allaa Y, Fahoumea M, Tite T, Galcab AC,Nouneh K. Charge storage mechanism and supercapacitive behavior of transparent vanadium pentoxide thin films in various aqueous electrolytes. *Results in Engineering.* 2025;28:107836.
[26] Ong KK, Zhang Y, Liao H, Jun HK, Liew CW. Unveiling the potential of BmImTFSI-functionalized poly (acrylic acid)-based ionogel polymer electrolyte for electrical double layer capacitor (EDLC) application. *Materials Science and Engineering: B.* 2026;327:119230.